Vietnam Journal of Science and Technology ***63*** *(3) (2025) 495-601*

doi:10.15625/2525-2518/18603

The effect of Zn doping concentration on thermoelectric properties of CuAgSe

Thi Huong Nguyen[1, *], Van Quang Nguyen[2], Duoc Phan Nguyen Duc[1], Sunglae Cho[3], Van Cuong Phan[1, *]

[1]*Department of Physics, Nha Trang University, Nha Trang 650000, Viet Nam*

[2]*Neutron Science Division, Korea Atomic Energy Research Institute, Daejeon 34057, Republic of Korea*

[3]*Department of Physics and Energy Harvest Storage Research Center, University of Ulsan, Ulsan 44610, Republic of Korea*

[*]Emails: *huongnt@ntu.edu.vn, cuongpv@ntu.edu.vn*

Received: 1 August 2023; Accepted for publication: 5 May 2025

Abstract. CuAgSe is a promising thermoelectric material due to its high carrier mobility and ultralow lattice thermal conductivity. In this work, Zn was doped into Cu sites at various concentrations (x = 0, 0.02, 0.04, 0.06, 0.08, and 0.10) to enhance its thermoelectric performance, resulting in compounds with the formula $Cu_{1-x}Zn_xAgSe$. The Zn-doped CuAgSe polycrystals were successfully synthesized using growth from the melt technique. The crystal structures of the samples were characterized by X-ray diffraction. The influence of Zn-doping on the thermoelectric properties was investigated in the temperature range of 300 - 673 K. Zn incorporation led to a reduction in lattice thermal conductivity to approximately 0.3 W m^{-1} K^{-1} at 673 K, along with an increase in electrical conductivity compared to undoped CuAgSe. Interestingly, the sample $Cu_{0.94}Zn_{0.06}AgSe$ exhibited the highest ZT of 0.69 at 673 K, approximately 3.5 times higher than that of the undoped material.

Keywords: Zn doping, CuAgSe, lattice thermal conductivity, thermoelectric materials

Classification numbers: 2.8.2, 2.10.2, 3.4.1.

1. INTRODUCTION

Global warming and energy shortages have spurred interest in clean, sustainable alternatives. Renewable sources, such as wind, hydro, and solar power, can replace fossil fuels, while industrial waste heat offers potential for energy recovery. Thermoelectric materials are promising for this purpose due to their stability, non-toxicity, and ability to directly convert heat into electricity using abundant elements [1]. The thermoelectric figure of merit (ZT), defined as $ZT=S^2\sigma T/\kappa$, evaluates a material's energy conversion efficiency, where S is the Seebeck coefficient, σ is electrical conductivity, κ is thermal conductivity, and absolute temperature (T). The term $S^2\sigma$, known as the power factor (PF), reflects the material's electrical performance [2].

High ZT requires a large PF and low κ [3]. Strategies to enhance ZT include band structure engineering, crystal structure modification, and impurity doping [4 - 6].

CuAgSe is a superionic compound and a promising candidate for thermoelectric applications. Similar to Cu_2Se, CuAgSe exhibits two temperature-dependent structural phases: a low-temperature β-phase and a high-temperature α-phase. Below 470 K, the β-CuAgSe phase exhibits an incommensurately modulated structure with an orthorhombic Pmmn(0β1/2)s00 superspace group and displays exceptionally high electron mobility, reaching approximately 56,000 cm² V¹ s¹ at 5 K [7]. This remarkable mobility reflects the good 'electron–crystal' transport behavior. Moreover, its complex structure and lattice disorder suggest glass- or liquid-like thermal transport characteristics. Above 470 K, CuAgSe transitions to the α- phase, adopting a face-centered cubic structure similar to the high-temperature superionic phase of Cu_2Se, where Ag^+/Cu^+ cations are randomly distributed within the Se^{2-} anions framework. This cationic disorder, exacerbated by partial Cu substitution with Ag, significantly lowers the lattice thermal conductivity, making it even lower than that of Cu_2Se [8, 9].

CuAgSe supports both n-type and p-type conduction with comparable ZT values, making it an ideal material for thermoelectric modules due to its matched thermal and mechanical properties. In recent years, several studies have reported on the thermoelectric performance of both n-type and p-type CuAgSe. Qiu *et al.* [10] achieved a maximum ZT of 0.7 at 450 K in n-type $CuAgSe_{0.95}Te_{0.05}$ by substituting Te at Se sites. Hong *et al.* [11] investigated p-type CuAgSe and reported a ZT of 0.95 at 623 K. Nguyen's group[12] introduced 2 % Zn into CuAgSe, resulting in a transition from p-type to n-type conduction and a ZT increase to 0.68 at 623 K. More recently, Yu *et al.* [13] demonstrated that Zn doping at the Cu sublattice in the CuAg-rich CuAgSe reduces vacancy concentrations, further improving thermoelectric performance, with ZT reaching 0.95 in $Cu_{1.01}Ag_{1.02}Zn_{0.01}Se$ (n-type). Despite these advances, a systematic investigation into the effect of Zn doping concentration on the thermoelectric properties of CuAgSe remains lacking.

In this study, Zn-doped CuAgSe materials with various doping concentrations were synthesized, and the effect of Zn content on their thermoelectric properties was systematically investigated. An ultralow lattice thermal conductivity of approximately 0.3 W m^{-1} K^{-1} at 673 K was achieved in the doped sample. The highest thermoelectric performance was observed in the $Cu_{0.94}Zn_{0.06}AgSe$ composition, which reached a maximum ZT value of 0.69 at 673 K, about 3.5 times higher than that of the undoped CuAgSe.

2. MATERIALS AND METHODS

Zn-doped CuAgSe polycrystalline samples were synthesized via the "growth from the melt" method using high-purity Cu, Ag, Se, Te, and Zn powders. Zn was substituted for Cu in $Cu_{1-x}Zn_xAgSe$ with doping levels ranging from 0 to 10 % (x = 0, 2, 4, 6, 8, and 10 %), as listed in Table 1. Powder mixtures were sealed in evacuated quartz ampoules, heated to 1323 K over 120 hours, held for 165 hours, then cooled to room temperature over 250 hours. The resulting ingots measured 13.5 mm in diameter and 25 mm in length. Phase analysis was performed using powder X-ray diffraction (XRD) (Rigaku Ultima IV, Cu Kα, λ = 1.54056Å, 2° min^{-1}). Bar-shaped samples (2 mm × 1.2 mm × 9 mm) were used for electrical conductivity and Seebeck coefficient measurements from 300 to 673 K under vacuum. Disk-shaped samples (ϕ14 mm × 2 mm) were prepared for thermal diffusivity (D) measurements via a Netzsch LFA-457. Mass density (ρ) was determined by the Archimedes method, and specific heat capacity (C_p) values were adopted from Hong *et al.* [11]. Total thermal conductivity (κ_{tot}) was calculated using the equation $\kappa_{tot} = DC_p\rho$.

Hall effect measurements were performed using a van der Pauw setup under a 0.45 T magnetic field. Estimated measurement uncertainties were ± 4.3 % (σ), ± 1.3 % (S), and 3 % (κ_{tot}).

3. RESULTS AND DISCUSSION

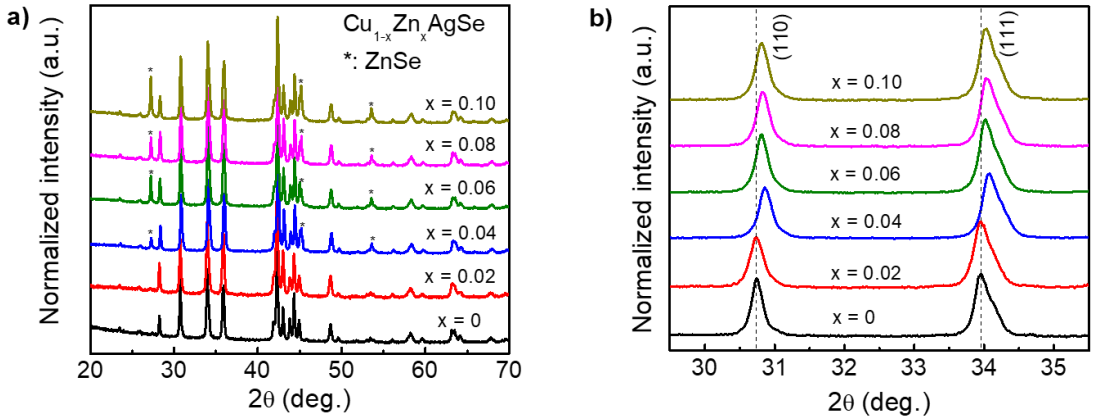

Figure 1. (a) XRD patterns for the $Cu_{1-x}Zn_xAgSe$ (x = 0 – 0.10) samples (b) enlarged XRD patterns in the 2θ angle range from 29.5° to 35.5° show a shift of (110) and (111) peaks.

XRD patterns of the $Cu_{1-x}Zn_xAgSe$ (x = 0 - 0.10) samples are shown in Figure 1 to examine their crystal structure. All samples exhibit nearly identical patterns, which are consistent with previously reported results [7, 14]. All observed peaks can be indexed to the incommensurately modulated CuAgSe phase with the superspace group *Pmmn*(0β1/2)s00. Secondary phase peaks corresponding to ZnSe appear when the Zn-doping content reaches x = 0.04, indicating that the solubility limit of Zn in the CuAgSe lattice is likely around 0.02. Figure 1(b) presents a magnified view of the XRD patterns in the 2θ range of 29.5°- 35.5° for all compositions. No noticeable peak shift is observed for $x \leq 0.02$. However, as the Zn content increases from x = 0.04 to x = 0.10, the (110) and (111) peaks gradually shift toward higher angles. This shift is attributed to the substitution of Cu^+ (ionic radius ~ 0.77 Å) with the slightly smaller Zn^{2+} ions (ionic radius ~ 0.74 Å), confirming the incorporation of Zn into Cu sites. These results confirm the successful synthesis of Zn-doped CuAgSe samples. The corresponding lattice parameters for each composition are listed in Table 1.

Table 1. Lattice constants, volume, mass density (which was obtained using the Archimedes method), carrier concentration, and carrier mobility at room temperature of $Cu_{1-x}Zn_xAgSe$ (x = 0 – 0.10) samples

Sample	**Lattice constants (Å)**			**Volume ($Å^3$)**	**Mass density (g/cm^3)**	**$n*10^{18}$ (cm^{-3})**	**μ ($cm^2 V^{-1} s^{-1}$)**
	a	**b**	**c**				
x = 0	4.096	4.050	6.326	104.926	7.827	4.575	2217
x = 0.02	4.097	4.049	6.328	104.968	7.819	7.699	4624
x = 0.04	4.085	4.039	6.310	104.113	7.694	9.728	2664
x = 0.06	4.090	4.044	6.317	104.471	7.586	8.327	3710
x = 0.08	4.087	4.042	6.314	104.327	7.457	9.048	2996
x = 0.10	4.089	4.045	6.317	104.478	7.565	9.820	2403

Figure 2 shows the temperature dependence of the Seebeck coefficient (*S*), electrical conductivity (σ), and power factor (*PF*) for $Cu_{1-x}Zn_xAgSe$ (x = 0 - 0.10) samples. In the undoped CuAgSe sample, the Seebeck coefficient exhibits an abrupt transition from negative to positive values around 470 K, corresponding to the known phase transition from the low-temperature β-phase to the high-temperature α-phase. In contrast, all Zn-doped samples maintain negative Seebeck coefficients across the entire temperature range, indicating stable n-type conduction with electrons as the dominant charge carriers. This behavior suggests that substituting Zn (which has two valence electrons) for Cu (which has one valence electron) introduces additional electrons into the system, thereby promoting n-type behavior. Moreover, the doped samples exhibit higher Seebeck coefficient values than the undoped samples at elevated temperatures. Notably, the $Cu_{0.94}Zn_{0.06}AgSe$ sample achieves the highest Seebeck coefficient of ~ 249 μV K^{-1} at 573 K.

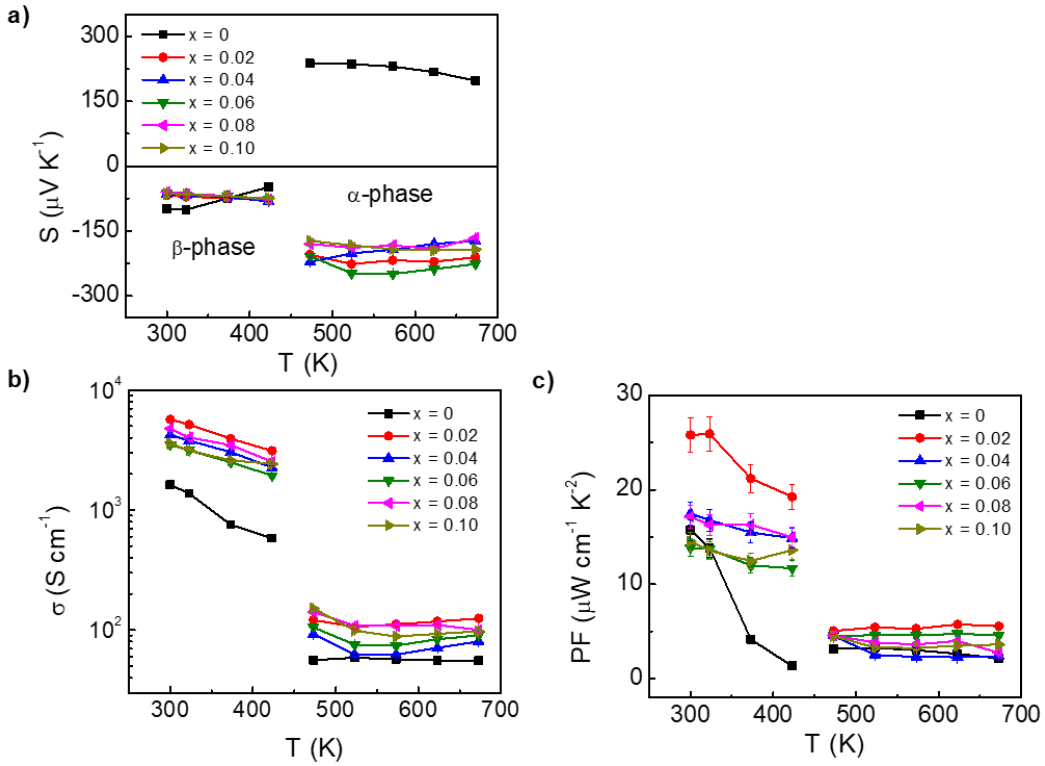

Figure 2. Temperature-dependent (a) Seebeck coefficient, (b) electrical conductivity, and (c) power factor of the $Cu_{1-x}Zn_xAgSe$ (x = 0 – 0.10) samples.

The variation of electrical conductivity versus temperature of the $Cu_{1-x}Zn_xAgSe$ (x = 0 – 0.10) samples is illustrated in Fig. 2b. For all compositions, electrical conductivity decreases with increasing temperature and exhibits a sharp drop above the phase transition temperature (~ 470 K), corresponding to the transition into the semiconducting α-phase. This behavior is consistent with the observed trends in the Seebeck coefficient. Interestingly, all Zn-doped samples show higher electrical conductivity than the undoped samples across the entire temperature ranges, which can be attributed to the additional free electrons introduced by Zn^{2+} substitution at Cu sites. The carrier concentration and mobility values at 300 K for each sample are provided in Table 1. Among the compositions, $Cu_{0.98}Zn_{0.02}AgSe$ exhibits the highest electrical conductivity, reaching 5697 S cm^{-1} at 300 K and 125 S cm^{-1} at 673 K due to its high carrier concentration and mobility. However, as the Zn doping content increases beyond x = 0.02, the electrical conductivity

gradually decreases. This reduction is likely due to the formation of the ZnSe secondary phase, which hinders carrier transport. These results suggest that moderate Zn doping can effectively enhance the electrical conductivity of CuAgSe, thereby improving its thermoelectric performance.

The calculated thermoelectric power factor ($PF = S^2\sigma$) as a function of temperature is presented in Figure 2c. Zn doping significantly enhances the PF due to simultaneous improvements in both the S and σ. At 300 K, the PF of the $Cu_{0.98}Zn_{0.02}AgSe$ sample reaches 25.8 μW cm^{-1} K^{-2}, roughly 1.64 times higher than that of undoped CuAgSe. As the temperature increases, the PF of all samples decreases in the α-phase region (T > 470 K), primarily due to the substantial drop in σ. Despite this decline, the $Cu_{0.98}Zn_{0.02}AgSe$ sample still exhibits the highest PF, with a maximum value of 5.8 μW cm^{-1} K^{-2} at 623 K, approximately 2.23 times greater than that of the pristine sample.

Figures 3a and 3b display the temperature dependence of thermal diffusivity (D) and total thermal conductivity (κ_{tot}) for all $Cu_{1-x}Zn_xAgSe$ samples. A similar trend was observed in the deviation D and κ_{tot} values. In the β-phase (T < 470 K), all samples show higher values of D and κ_{tot} compared to those in the α-phase. As temperature increases within the β-phase, both parameters gradually decrease, while in the α-phase (T > 470 K), a slight increase is observed. This behavior is primarily attributed to enhanced phonon-phonon scattering at elevated temperatures in the α-phase. Moreover, Zn-doped samples present lower D and κ_{tot} values than the undoped sample across the entire temperature range, which can ascribed to increased phonon scattering induced by mass and strain field fluctuations introduced by the Zn dopants.

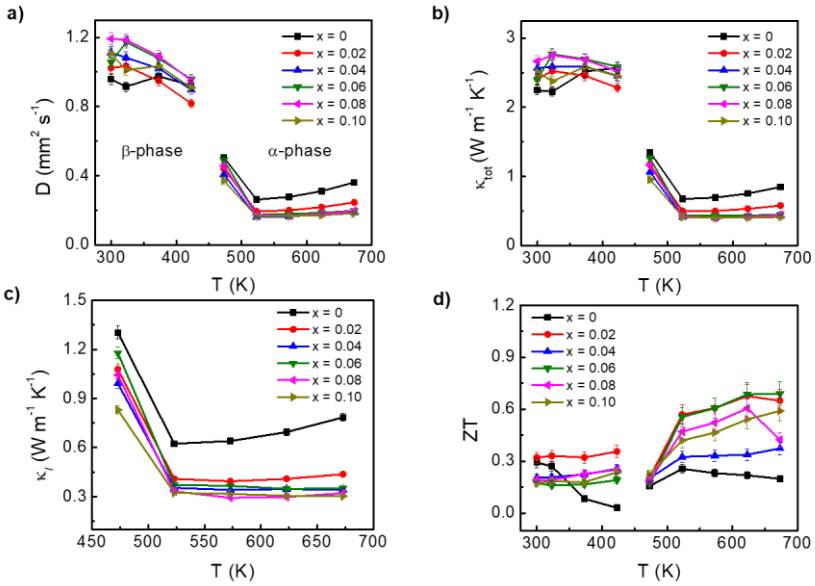

Figure 3. Temperature dependence of (a) thermal diffusivity, (b) total thermal conductivity, (c) lattice thermal conductivity, and (d) ZT for the $Cu_{1-x}Zn_xAgSe$ (x = 0 – 0.10) samples.

To gain deeper insight into the temperature dependence of thermal conductivity, the lattice thermal conductivity (κ_l) was determined by subtracting the electronic thermal conductivity (κ_e) from the total thermal conductivity (κ_{tot}). The κ_e values were calculated using the Wiedemann-Franz law: $\kappa_e = L\sigma T$, where L is the Lorentz number. Under the single parabolic band model assumption, L is estimated using the empirical relation $L\,[10^{-8}V^2K^{-2}] = 1.5 + exp\{-|S|/116\}$,

where S is the measured Seebeck coefficient. The calculated Lorentz number ranged from 1.62 to 2.16 × 10^{-8} V^2 K^{-2}, as detailed in the Supplementary Information. As shown in Fig. 3c, κ_l decreases systematically with increasing Zn doping concentration, which can be attributed to enhanced phonon scattering introduced by Zn dopants. Interestingly, the $Cu_{0.9}Zn_{0.10}AgSe$ sample exhibits the lowest κ_l values of 0.3 W m^{-1} K^{-1} at 673 K, representing a 2.6-fold reduction compared to undoped CuAgSe.

Figure 3d presents the temperature dependence of the ZT for both pristine and Zn-doped CuAgSe samples. Higher ZT values are observed in the high-temperature α-phase compared to the low-temperature β-phase, primarily due to the significantly lower total thermal conductivity in the α-phase. The enhancement in ZT with Zn doping is mainly attributed to the increase in electrical conductivity resulting from the elevated carrier concentration introduced by Zn substitution. Among all samples, $Cu_{0.94}Zn_{0.06}AgSe$ exhibits the highest ZT value of 0.69 at 673 K, representing an improvement of about 245 % compared to undoped CuAgSe.

4. CONCLUSIONS

In this study, a series of Zn-doped CuAgSe samples were successfully synthesized using growth from the melt method. The crystal structure and electrical and thermal transport properties of the samples were systematically investigated. XRD analysis revealed that the Zn solubility limit in β-CuAgSe is around 0.02. Compared to the undoped CuAgSe sample, Zn doping effectively enhanced electrical conductivity by increasing carrier concentrations while simultaneously reducing the lattice thermal conductivity to as low as 0.3 W m^{-1} K^{-1} at 673 K. A maximum ZT value of 0.69 was achieved at 673 K for the $Cu_{0.94}Zn_{0.06}AgSe$ sample. These results demonstrate that Zn doping is a promising strategy for tuning carrier concentration and optimizing the thermoelectric performance of CuAgSe.

Acknowledgments. The authors gratefully acknowledge Dr. Jong-Ho Park and Prof. Su-Dong Park (Thermoelectric Conversion Research Center, Korea Electrotechnology Research Institute, Korea) for support of thermal diffusivity measurement.

CRediT authorship contribution statement. Thi Huong Nguyen: Conceptualization, Methodology, Investigation, Writing – Original Draft. Van Quang Nguyen: Investigation, Visualization. Duoc Phan Nguyen Duc: Investigation. Sunglae Cho: Resources, Supervision. Van Cuong Phan: Writing – Review & Editing, Supervision.

Declaration of competing interest. The authors declare that they have no known competing financial interests or personal relationships that could have appeared to influence the work reported in this paper.

REFERENCES

1. Hendricks T., Caillat T., and Mori T. - Keynote review of ratest advances in thermoelectric generation materials, devices, and technologies 2022, Energies **15** (19) (2022) 7307. https://doi.org/10.3390/en15197307.
2. Biswas K., Ren Z., Grin Y., Lee K. H., Mori T., and Chen L. - Thermoelectric materials science and technology toward applications, Appl. Phys. Lett. **121** (2022) 070401. https://doi.org/10.1063/5.0115322.
3. Tan G., Ohta M., and Kanatzidis M. G. - Thermoelectric power generation: From new materials to devices, Philos. Trans. R. Soc. A **377** (2019) 20180450. https://doi.org/10.1098/rsta.2018.0450.

4. Xiao Y. and Zhao L. D. - Charge and phonon transport in PbTe-based thermoelectric materials, npj Quant. Mater. **3** (2018) 55. https://doi.org/10.1038/s41535-018-0127-y.

5. Pei Y. L., Wu H., Wu D., Zheng F., and He J. - High thermoelectric performance realized in a BiCuSeO system by improving carrier mobility through 3D modulation doping, J. Am. Chem. Soc. **136** (2014) 13902-13908. https://doi.org/10.1021/ja507945h.

6. Qian X., Wu H., Wang D., Zhang Y., Wang J., Wang G., Zheng L., Pennycook S. J., and Zhao L. D. - Synergistically optimizing interdependent thermoelectric parameters of n-type PbSe through alloying CdSe, Energy Environ. Sci. **12** (2019) 1969-1978. https://doi.org/10.1039/c8ee03386b.

7. Yang Q., Ming C., Qiu P., Zhou Z., Qiu X., Gao Z., Deng T., Chen L., and Shi X. - Incommensurately modulated structure in AgCuSe-based thermoelectric materials for intriguing electrical, thermal, and techanical properties, Small (2023) 2300699. https://doi.org/10.1002/smll.202300699.

8. Zuo Y., Liu Y., He Q. P., Song J. M., Niu H. L., and Mao C. J. - CuAgSe nanocrystals: Colloidal synthesis, characterization and their thermoelectric performance, J. Mater. Sci. **53** (2018) 14998-15008. https://doi.org/10.1007/s10853-018-2676-7.

9. Wang X., Qiu P., Zhang T., Ren D., Wu L., Shi X., Yang J., and Chen, L. - Compound defects and thermoelectric properties in ternary CuAgSe-based materials, J. Mater. Chem. A **3** (2015) 13662-13670. https://doi.org/10.1039/c5ta02721g.

10. Qiu P. F., Wang X. B., Zhang T. S., Shi X., and Chen, L. D. - Thermoelectric properties of Te-doped ternary CuAgSe compounds, J. Mater. Chem. A **3** (2015) 22454-22461. https://doi.org/10.1039/c5ta06780d.

11. Hong A. J., Li L., Zhu H. X., Zhou X. H., He Q. Y., Liu W. S., Yan Z. B., Liu J. M., and Ren Z. F. - Anomalous transport and thermoelectric performances of CuAgSe compounds, Solid State Ionics **261** (2014) 21-25. https://doi.org/10.1016/j.ssi.2014.03.025.

12. Nguyen T. H., Nguyen V. Q., Pham A. T., Park J. H., Lee J. E., Lee J. K., Park S., and Cho, S. - Carrier control in CuAgSe by growth process or doping, J. Alloys Compd. **852** (2021) 157094. https://doi.org/10.1016/j.jallcom.2020.157094.

13. Yu T., Ning S., Liu Q., Zhang T., Chen X., Qi N., Su X., Tang X., and Chen Z. - Balanced high thermoelectric performance in n-type and p-type CuAgSe realized through vacancy manipulation, ACS Appl. Mater. Interfaces **15** (2023) 40781-40791. https://doi.org/ 10.1021/acsami.3c08897

14. Nguyen T. H., Nguyen V. Q., Park J. H., Tran T. T., Pham A. T., Park S., Rhyee J. S., and Cho S. - Raising n-type thermoelectric performance in (Te, Zn)-codoped CuAgSe, ACS Appl. Energy Mater. **6** (2023) 6151-6156. https://doi.org/10.1021/acsaem.3c00683